

Preparation and Tribological Properties of Graphene Lubricant Additives for Low-Sulfur Fuel by Dielectric Barrier Discharge Plasma-Assisted Ball Milling

Authors:

Xianbin Hou, Yanjun Ma, Geetanj Bhandari, Zibin Yin, Leyang Dai, Haifeng Liao, Yukun Wei

Date Submitted: 2022-11-01

Keywords: low-sulfur fuel, graphene, lubricant additive, lubrication property, surface modification, dielectric barrier discharge plasma-assisted ball milling

Abstract:

Poor lubrication performance of low-sulfur fuel leads to increased wear of diesel engine components. In order to improve the lubrication properties of low-sulfur fuel, we successfully prepared graphene lubricant additives by dielectric barrier discharge plasma-assisted ball milling. The tribological properties of graphene lubricant additives in two types of 0# diesel oils with different sulfur content were evaluated by high-frequency reciprocating rig (HFRR). The results indicated that the expanded graphite was exfoliated and refined into graphene sheets with nine layers by the synergistic effect of the heat explosive effect of the discharge plasma, the impact of mechanical milling function, and the cavitation effect of 0# diesel oil. The organic functional groups of 0# diesel oil were successfully grafted on the surface of graphene sheets. The addition of 0.03 wt % graphene resulted in 20% reduction in the friction coefficient (COF) and 28% reduction in wear scar diameter (WSD) compared to pure 0# diesel oil with a sulfur content of 310 mg/kg. The addition of 0.03 wt % graphene resulted in 24% reduction in the friction coefficient (COF) and 30% reduction in wear scar diameter (WSD) compared to pure 0# diesel oil with a sulfur content of 1.1 mg/kg. The formation of graphene tribofilm on rubbing surfaces improved the lubrication properties of low-sulfur fuel.

Record Type: Published Article

Submitted To: LAPSE (Living Archive for Process Systems Engineering)

Citation (overall record, always the latest version):

LAPSE:2022.0122

Citation (this specific file, latest version):

LAPSE:2022.0122-1

Citation (this specific file, this version):

LAPSE:2022.0122-1v1

DOI of Published Version: <https://doi.org/10.3390/pr9020272>

License: Creative Commons Attribution 4.0 International (CC BY 4.0)

Article

Preparation and Tribological Properties of Graphene Lubricant Additives for Low-Sulfur Fuel by Dielectric Barrier Discharge Plasma-Assisted Ball Milling

Xianbin Hou ^{1,2}, Yanjun Ma ¹, Geetanj Bhandari ³ , Zibin Yin ¹, Leyang Dai ^{1,*} , Haifeng Liao ¹ and Yukun Wei ¹

¹ School of Marine Engineering, Jimei University, Xiamen 361021, China; 201914824002@jmu.edu.cn (X.H.); 201912852025@jmu.edu.cn (Y.M.); 199561000007@jmu.edu.cn (Z.Y.); 199961000050@jmu.edu.cn (H.L.); max@jmu.edu.cn (Y.W.)

² School of Marine Technology, Beibu Gulf University, Qinzhou 535011, China

³ Geetanj Bhandari, Rtec Instruments Inc., San Jose, CA 95131, USA; geetanj@rtec-instruments.com

* Correspondence: daileyang@jmu.edu.cn

Abstract: Poor lubrication performance of low-sulfur fuel leads to increased wear of diesel engine components. In order to improve the lubrication properties of low-sulfur fuel, we successfully prepared graphene lubricant additives by dielectric barrier discharge plasma-assisted ball milling. The tribological properties of graphene lubricant additives in two types of 0# diesel oils with different sulfur content were evaluated by high-frequency reciprocating rig (HFRR). The results indicated that the expanded graphite was exfoliated and refined into graphene sheets with nine layers by the synergistic effect of the heat explosive effect of the discharge plasma, the impact of mechanical milling function, and the cavitation effect of 0# diesel oil. The organic functional groups of 0# diesel oil were successfully grafted on the surface of graphene sheets. The addition of 0.03 wt % graphene resulted in 20% reduction in the friction coefficient (COF) and 28% reduction in wear scar diameter (WSD) compared to pure 0# diesel oil with a sulfur content of 310 mg/kg. The addition of 0.03 wt % graphene resulted in 24% reduction in the friction coefficient (COF) and 30% reduction in wear scar diameter (WSD) compared to pure 0# diesel oil with a sulfur content of 1.1 mg/kg. The formation of graphene tribofilm on rubbing surfaces improved the lubrication properties of low-sulfur fuel.

Keywords: low-sulfur fuel; graphene; lubricant additive; lubrication property; surface modification; dielectric barrier discharge plasma-assisted ball milling



Citation: Hou, X.; Ma, Y.; Bhandari, G.; Yin, Z.; Dai, L.; Liao, H.; Wei, Y. Preparation and Tribological Properties of Graphene Lubricant Additives for Low-Sulfur Fuel by Dielectric Barrier Discharge Plasma-Assisted Ball Milling. *Processes* **2021**, *9*, 272. <https://doi.org/10.3390/pr9020272>

Received: 26 December 2020

Accepted: 28 January 2021

Published: 31 January 2021

Publisher's Note: MDPI stays neutral with regard to jurisdictional claims in published maps and institutional affiliations.



Copyright: © 2021 by the authors. Licensee MDPI, Basel, Switzerland. This article is an open access article distributed under the terms and conditions of the Creative Commons Attribution (CC BY) license (<https://creativecommons.org/licenses/by/4.0/>).

1. Introduction

Sulfur oxides (SOX), which are the main pollutant of air pollution and environmental acidification, are part of exhaust emissions from marine diesel engines. The problem of air pollution is becoming more and more serious, arousing wide public concern [1,2]. To control exhaust pollution from marine diesel engines, the International Maritime Organization (IMO) issued Supplement VI of MARPOL Convention-Rules for preventing air pollution from vessels. Since 1 January 2020, the sulfur content of fuel used by marine diesel engines has been reduced from 3.5% to 0.5% even outside SOX emission control area (SECA) [3]. However, the desulfurization process of fuel removes some of the polar bonds that are useful for their lubricating properties. The removal of polar compounds will even significantly deteriorate the lubricity of ultra-low sulfur diesel [4], which will cause a large number of problems, including excessive and rapid wear of the fuel pump, fuel injection nozzle corrosion, complex engine start-up, engine instability, insufficient engine power, and shortened life span of the engine [5].

At present, the way in which to improve the lubricity of low-sulfur fuel has attracted the interest of researchers. Addition of lubricating additives to low-sulfur fuel is an effective method to improve the lubricity of low-sulfur fuel. Hu et al. added the high oil fatty

acid to ultra-low sulfur non-additive 0# diesel as an anti-wear agent, wherein the wear scar diameter and the coefficient of friction were reduced by 60.3% and 95.7%, respectively [6]. Soybean oil and other vegetable oils were researched as raw material to synthesize monoethanolamides as lubricating additives for low-sulfur marine fuel, and the average wear scar diameter (WS 1.4) was less than 520 μm when the concentration of monoethanolamides was 80–140 ppm [7]. Tomic et al. conducted research using biodiesel oil obtained from sunflower oil as an additive and added it to low-sulfur diesel oil (fossil diesel oil) with a volume ratio of 3%, finding that the lubrication properties of low-sulfur diesel oil were significantly improved and the wear scar diameter was reduced by 42% [8]. Sun et al. developed biochar-based lubricating additives for low-sulfur diesel fuel and found the average wear scar diameter values of low-sulfur diesel fuel decreased progressively with the increase of additive concentration [9]. Liu et al. synthesized tung oil-based fatty acid methyl ester and the maleation compound as lubricating additive for ultralow-sulfur diesel fuel—the wear scar and friction of ultralow-sulfur diesel fuel were reduced by 40 and 46–47% with low additive levels of 500 ppm and 1000 ppm, respectively [10]. However, these additives have poor compatibility with low-sulfur fuel and cause different degrees of pollution to low-sulfur fuel. Therefore, the development of simple, low-cost, pollution-free lubricating additives for low-sulfur fuel has become the goal of researchers.

Graphene has an atomically thin thickness and a layered structure with low shear strength, high mechanical strength, low surface energy, and chemical stability in harsh environments [11], which make graphene widely studied as a lubricant additive [12,13]. Wang et al. prepared graphene with 4–6 layers in size of 3–5 μm by liquid phase exfoliation method and then dispersed it into SAE 10W-30 (SAE is the abbreviation of Society of Automotive Engineers. SAE grade represents the viscosity grade of oil) lubricating oil with the concentration of 0.05 wt %, finding that the coefficient of friction and specific wear rate were reduced by 65% and 66%, respectively [14]. Gayatri et al. prepared the dodecyl amine functionalized graphene (DAG) by solution mixing and found that addition of 0.10 wt % DAG into 5W-30 resulted in 40% reduction of friction coefficient [15].

However, graphene shows incompatibility with most solvents/lubricants and tends to agglomerate due to high cohesion interactions [11]. The long-term dispersion stability of graphene in lubricants has been a major challenge for the lubricant industry—researchers either functionalize graphene or use dispersants to stably disperse graphene in traditional lubricants, but the process of preparing functionalized graphene is complex.

Dielectric barrier discharge plasma-assisted ball milling (DBDP-assisted ball milling) is a novel preparation method of nano lubricant additives [16]. Yan et al. prepared surface-modified nano-TiO₂ powders of about 20 nm with quaternary ammonium salt and lauric acid sodium salt as surface modifier by DBDP-assisted ball milling for 11 h, and the results showed that plasma made quaternary ammonium salt and lauric acid sodium salt more prone to broken bonds and polymerization and promoted the surface modification of TiO₂ powders, which were well dispersed in 40 CA (CA stands for diesel engine oil). marine lubricating oil and possessed excellent tribological properties [17].

In this paper, in order to improve the lubrication properties of low-sulfur fuel, we prepared surface-modified graphene lubricant additives for low-sulfur fuel by DBDP-assisted ball milling, with expanded graphite as raw material and 0# diesel oil as surface modifier. The microstructure, dispersity, and physicochemical properties of the graphene additives were tested and analyzed by different means. The tribological properties of graphene additives in 0# diesel oils with different sulfur content were investigated by high-frequency reciprocating rig (HFRR), and the mechanism of friction reduction and anti-wear was analyzed. This study can provide a method for improvement of low-sulfur fuel lubrication properties, which has important practical value for commercial application of graphene.

2. Materials and Methods

2.1. Materials

Expanded graphite was obtained from unexpanded graphite. Unexpanded graphite was purchased from Shanghai Yifang Graphite Co., Ltd (Shanghai, China). The unexpanded graphite was heated to 1000 °C in a chamber electric furnace (SX2-4-10, Luoyang Zipu Furnace Co., Ltd., Luoyang, China) with 4 kW power and was kept at 1000 °C for 20 min. After cooling to room temperature, the resulting expanded graphite was obtained. The 0# diesel oil with a sulfur content of 310 mg/kg (named oil sample 1) and 0# diesel oil with a sulfur content of 1.1 mg/kg (named oil sample 2) were purchased from PetroChina Company Limited (Xiamen, China). The physical and chemical properties of 0# diesel oil used in this experiment are shown in Table 1.

Table 1. Physical and chemical properties of 0# diesel oil.

Fuel Oil Type	Sulfur Content (mg/kg)	Closed Flash Point (°C)	Kinematic Viscosity (20 °C) (mm ² /s)
0# diesel oil with a sulfur content of 310 mg/kg (oil sample 1)	310	66	4.7998
0# diesel oil with a sulfur content of 1.1 mg/kg (oil sample 2)	1.1	72	3.06

2.2. Synthesis of Graphene Lubrication Additives

Expanded graphite (5 g) and 0# diesel oil (oil sample 1) (500 mL) were mixed evenly and put into DBDP-assisted ball milling tank (Sunwoda Electronic Co., Ltd. Shenzhen, China). The mill balls were 6, 4, 2, and 1 mm in diameter. DBDP-assisted ball milling was carried out on a self-made DBDP-assisted ball milling device, as shown in Figure 1. The vibration frequency of the device was 16 Hz and the amplitude was 10 mm. DBDP-assisted ball milling tank was filled with 0.1 MPa argon gas. The plasma discharge voltage was 23 kV, the electric current was 1.5 A, and the discharge frequency was 60 kHz. Graphene lubrication additives (fuel modified graphene) were obtained by DBDP-assisted ball milling for 10 h.

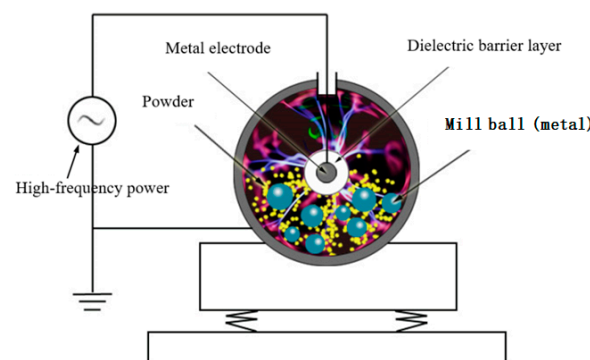


Figure 1. Schematic design of dielectric barrier discharge plasma-assisted ball milling.

2.3. Fuel Lubrication Properties Tests

A certain amount of graphene additives was added into 0# diesel oil (oil sample 1 and oil sample 2). The lubricity of graphene additives in 0# diesel oil (oil sample 1 and oil sample 2) were evaluated via high-frequency reciprocating rig (HFRR). The friction and wear were measured under boundary lubrication conditions using a highly stressed ball-on-disc contact (ball-AISI 52100 bearing steel, D = 6 mm, hardness 700 HV, and Ra 0.018 µm; disk-AISI 52100 bearing steel, φ = 20 mm, h = 3.5 mm, hardness 700 HV, and Ra 0.018 µm). The upper ball makes high-frequency short stroke reciprocating motion under a certain load, while the lower disc is fixed in the oil box. The steel ball slides on the steel

disc, and the contact part of the upper ball and lower disc is completely immersed in the test diesel fuel.

The effect of graphene additives on the lubricity of 0# diesel oil (oil sample 1 and oil sample 2) was evaluated according to the ISO12156-1:1997, and the test conditions were selected as follows: diesel oil temperature was 60 °C, testing mass was 200 g, frequency was 50 Hz, stroke length was 1.0 mm, testing duration was 75 min. In order to minimize any outside interference during tests, we controlled both the humidity and temperature. At the end of the test, the wear scar diameter (WSD) of the ball was measured at the optical microscopy. The WSD was corrected to normalize vapor pressure to 1.4 kPa. At the same time, the average value of friction coefficient (COF) was obtained.

2.4. Characterization

The samples were characterized by standard available characterization techniques. Field emission scanning electron microscopy (FESEM, ZEISS VEO 18, Carl Zeiss AG, Germany), high-resolution transmission electron microscopy (HRTEM, TECNAI G230S-TWIN, FEI, Hillsboro, OR, USA), Raman spectroscopy (HREvolution, HORIBA Jobin Yvon, Paris, France), and XRD (MiniFlex600, Rigaku Corporation, Japan) were used to characterize the microstructure and chemical composition of the sample. FTIR (NICOLET IS10, Thermo Nicolet Corporation, Madison, WI, USA) was employed to confirm the chemical groups of the sample surface. Energy-dispersive spectroscopy (EDS, Hitachi model SU8010, HITACHI, Japan) was employed to investigate the chemical composition of the tribo-film on the wear zones. The sulfur content of 0# diesel oil was measured by Oil Sulfur Analyzer (KL3120, Shanghai Yutong Instrument Factory, Shanghai, China). The closed flash point of 0# diesel oil was examined by full automatic closed cup flash point tester (DZY-002Z, Dalian Instruments And Meters Co., Ltd, Dalian, China). The kinematic viscosity of 0# diesel oil was analyzed by stabinger viscometer (SVM 3001, Anton Paar, Austria). The calorific value of 0# diesel oil was measured by calorific value meter (DZY-RIA, Dalian Instruments And Meters Co., Ltd., Dalian, China). The atomization performance of 0# diesel oil was analyzed by comprehensive calibrator for injectors and nozzles (BD-PQZ, Taian Kechuang Experimental Equipment Co., Ltd., Taian, China).

3. Results and Discussion

3.1. Characterization of Fuel Modified Graphene

Figure 2 shows the images of expanded graphite (before DBDP-assisted ball milling) and fuel modified graphene (after DBDP-assisted ball milling). The SEM image in Figure 2a shows that the expanded graphite was the lamellar structure and closely agglomerated together before DBDP-assisted ball milling. As seen in the SEM image in Figure 2b, fuel-modified graphene sheets were broken and exfoliated, and loosely stacked together after DBDP-assisted ball milling for 10 h. It seems that the fuel-modified graphene sheets had better dispersion compared with the expanded graphite sheets before DBDP-assisted ball milling.

Figure 3 shows the micrograph of the fuel-modified graphene after DBDP-assisted ball milling for 10 h. As shown in Figure 3a, the graphene sheets were transparent and in corrugated shapes. Figure 3a clearly reveals the ultrathin structure and smooth surface of the fuel-modified graphene. This was essential to ensure that the fuel-modified graphene sheets inserted into the friction pairs. It can be observed in Figure 3b that the graphene sheets were obviously layered aggregation. As shown by the arrow in Figure 3b, it was possible to observe nine well-ordered stacking layers that were typical of multilayer graphene.

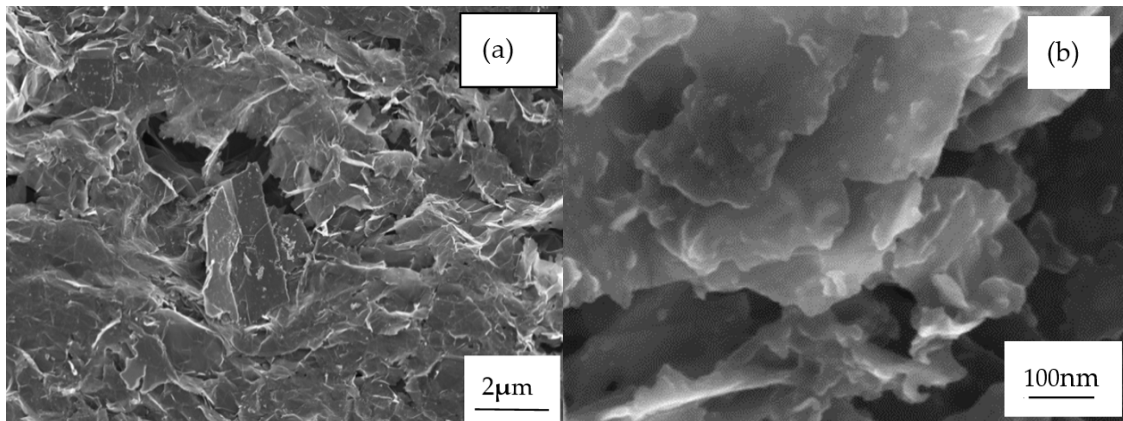


Figure 2. SEM images of (a) the expanded graphite and (b) fuel-modified graphene.

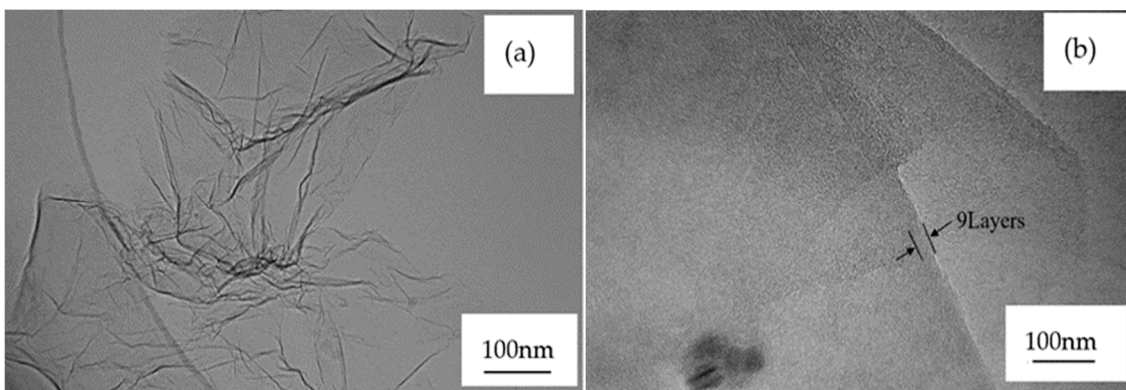


Figure 3. TEM images of fuel-modified graphene. (a) The micrograph of graphene after DBDP-assisted ball milling for 10 h; (b) The graphene sheets after DBDP-assisted ball milling for 10 h.

The XRD patterns of expanded graphite (before DBDP-assisted ball milling) and fuel-modified graphene (after DBDP-assisted ball milling) are presented in Figure 4. A sharp diffraction peak in the XRD pattern of expanded graphite was located at $2\theta = 26.5^\circ$, which can be attributed to the contribution of (002) crystal plane of hexagonal graphite. A diffraction peak of fuel-modified graphene was located at $2\theta = 26.3^\circ$. The diffraction peak at 26° was assigned to the stacking of graphene sheets [18,19]. Obviously, the diffraction peak of fuel modified graphene was weakened dramatically in comparison with that of the expanded graphite, indicating that the expanded graphite tended to be amorphous and a downsizing phenomenon occurred after DBDP-assisted ball milling [20]. At the same time, the position of the diffraction peak of fuel-modified graphene shifted slightly to the left in comparison with that of the expanded graphite, which means that interlayer spacing increased after DBDP-assisted ball milling.

The Raman spectra of expanded graphite and fuel-modified graphene are presented in Figure 5. Three peaks were observed at ≈ 1350 , ≈ 1580 , and ≈ 2700 cm^{-1} , which are called D band, G band, and 2D band, respectively. The D band at ≈ 1350 cm^{-1} is attributed to the disordered carbon, the G band at ≈ 1580 cm^{-1} is attributed to the characteristic peak of the in-plane vibration of a layer of sp^2 carbon atoms, and the 2D band at ≈ 2700 cm^{-1} arises from a two-phonon double-resonance Raman process [21,22]. The ratio of intensities I_D/I_G can be used to define the graphitization degree of carbon materials [23]. The I_D/I_G value (0.2) of the fuel-modified graphene was higher than that of the expanded graphite (0.14), showing that the layer number of graphite material decreased after 10 h ball milling. The result was in consistency with the analysis of TEM in Figure 3, with the number of graphene layers being decreased to nine.

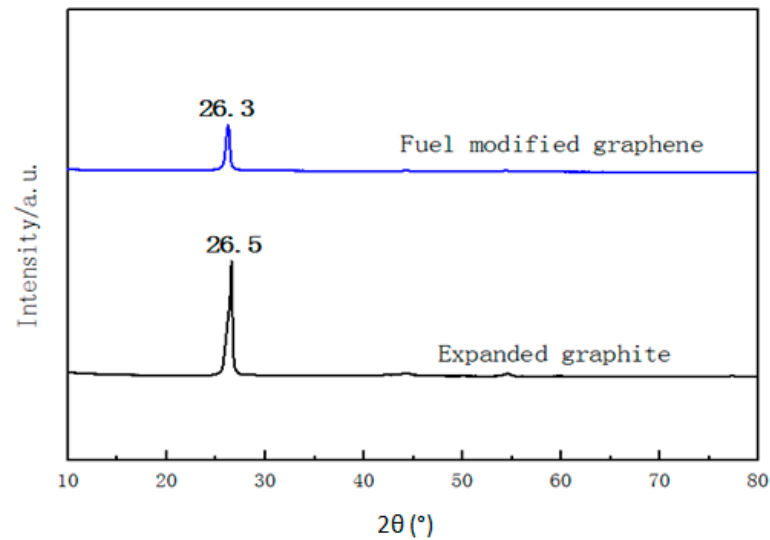


Figure 4. XRD patterns of expanded graphite and fuel-modified graphene.

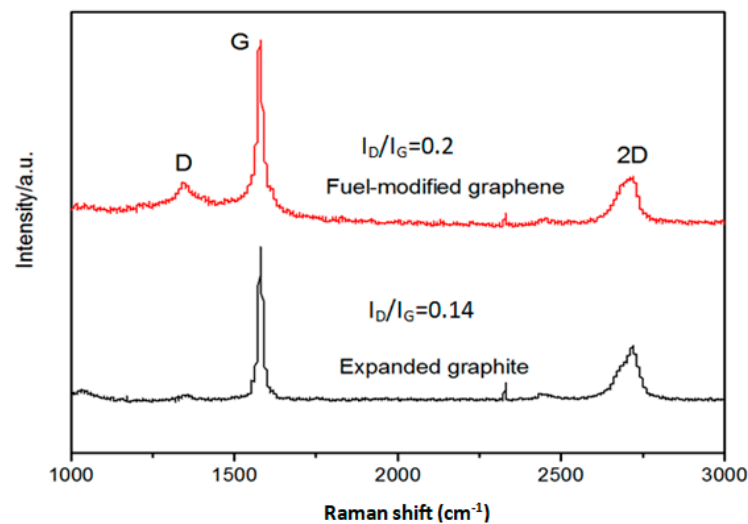


Figure 5. Raman spectra of expanded graphite and fuel-modified graphene.

Figure 6 shows the FTIR spectra of expanded graphite and fuel-modified graphene. The spectrum of the expanded graphite presents the following peaks. The peak at 3153 cm^{-1} is attributed to the stretching vibration of the O–H group [24]. The band at 1584 cm^{-1} is attributed to the C=C stretching vibration peak [25]. The band at 1400 cm^{-1} is attributed to the tertiary C–OH groups. The band at 1052 cm^{-1} is attributed to the C–C vibration peak in the benzene ring structure of the graphite crystal. On the spectra of the fuel-modified graphene, the spectrum at 3462 cm^{-1} is attributed to stretching vibration of –OH, which should be the hydroxyl of the 0# diesel oil grafted on the surface of the graphene sheets. The peaks at 2924 cm^{-1} and 2850 cm^{-1} are attributed to the stretching vibration of –CH₂ and –CH₃, which come from the organic functional groups of low-sulfur fuel [26]. The peaks at 1688 cm^{-1} and 1374 cm^{-1} are assigned to stretching vibration of C=C and absorption peak of C–H, which come from the organic functional groups of 0# diesel oil. According to the analysis of FTIR spectra, we can preliminarily conclude that the organic functional groups of 0# diesel oil were successfully grafted on the surface of the graphene sheets. With the intercalation of the hydrocarbon long chains between the layers, the fuel-modified graphene sheets were prevented from agglomerating. They were loosely stacked. The result is in consistency with the analysis of SEM in Figure 2.

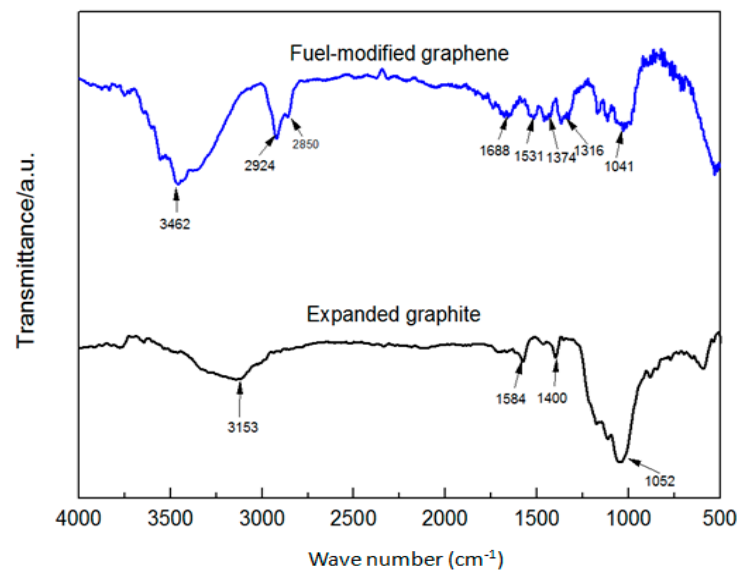


Figure 6. FTIR spectra of expanded graphite and fuel-modified graphene.

3.2. The Dispersion of Graphene Additives in 0# Diesel Oil

Stable dispersibility in 0# diesel oil as a nano-lubricant additive is very important for graphene. It is essential to guarantee the excellent lubricating property of graphene additives. To monitor the stability of graphene additives in 0# diesel (oil sample 1), we carried out dispersion analysis. Figure 7 shows different concentrations of graphene additives dispersed in 0# diesel oil (oil sample 1) after ultrasonic treatment for 30 min. After 20 days of storage, the 0# diesel oil with 0.01 wt %, 0.02 wt %, and 0.03 wt % of graphene additives had good dispersibility. This can be attributed to the hydrocarbon long chains grafted to the graphene additive surfaces—the graphene additives had good compatibility with 0# diesel oil (oil sample 1). However, while the amount of graphene additives was greater than 0.03 wt %, the oil sample showed a precipitation phenomenon. Because graphene has a large specific surface area and high surface energy, it is easier to adsorb and agglomerate together when the amount of graphene additives increases.

3.3. Preparation and Modification Mechanisms

When graphene lubricant additive is prepared by DBDP-assisted ball milling, the expanded graphite is broken and exfoliated by the impact and shear of the milling balls. At the same time, the high-temperature plasma heats the graphite to promote the expansion and exfoliation of graphite sheets. On the other hand, high-density and high-energy plasma bombards the surface of graphite sheets and fuel, producing a huge impact force, which not only accelerates the refinement and exfoliation of graphite sheets, but also causes part of fuel to evaporate and gasify, which leads to fuel sputtering on graphite and causes cavitation effects [27,28]. Part of the sputtering fuel is embedded between the graphite sheets and accelerates the exfoliation of the graphite sheets. During the cavitation process, a large amount of energy is released by the bubbles when they burst. The energy has a strong impact on the graphite sheets, which further accelerates the refinement and exfoliation of the graphite sheets. During DBDP-assisted ball milling, the plasma will make some high molecular polymers more prone to broken bonds and polymerization [29]. At the same time, when the cavitation occurs, the local temperature and pressure increase sharply when the bubble bursts, which results in decomposition and broken bonds of fuel molecules, generating free radicals and promoting chemical reactions [27,30], as well as the production of a large number of organic functional groups ($-\text{OH}$, $\text{C}=\text{C}$, $-\text{CH}_3$, $-\text{CH}_2$, $\text{C}-\text{H}$). The highly active particles (ions, electrons, atoms, and molecules in an excited state; free radicals; etc.) produced by plasma are easy to adsorb with the graphene sheets, which results in the increase of surface activity of the graphene sheets, as well as the fresh surfaces, and a large

number of defects introduced by DBDP-assisted ball milling further enhances the activity of the graphene sheets, which makes diffusion, phase transition, and chemical reaction easier. The organic functional groups ($-\text{OH}$, $\text{C}=\text{C}$, $-\text{CH}_3$, $-\text{CH}_2$, $\text{C}-\text{H}$) of the 0# diesel oil (oil sample 1) are absorbed or polymerized on the surface of the graphene sheets. Owing to the synergism of the thermal explosion effect produced by plasma, the mechanical impact effect produced by DBDP-assisted ball milling, and cavitation effect produced by fuel, in our study, expanded graphite was exfoliated and refined into graphene sheets with nine layers. At the same time, the organic functional groups ($-\text{OH}$, $-\text{CH}_2$, $-\text{CH}_3$, $\text{C}=\text{C}$, $\text{C}-\text{H}$) of 0# diesel oil (oil sample 1) were adsorbed or polymerized on the surface of the graphene sheets, and the hydrocarbon long-chain structure similar to that of 0# diesel oil (oil sample 1) was formed on the surface of the graphene sheets. Graphene lubricant additives had good compatibility with 0# diesel oil (oil sample 1).

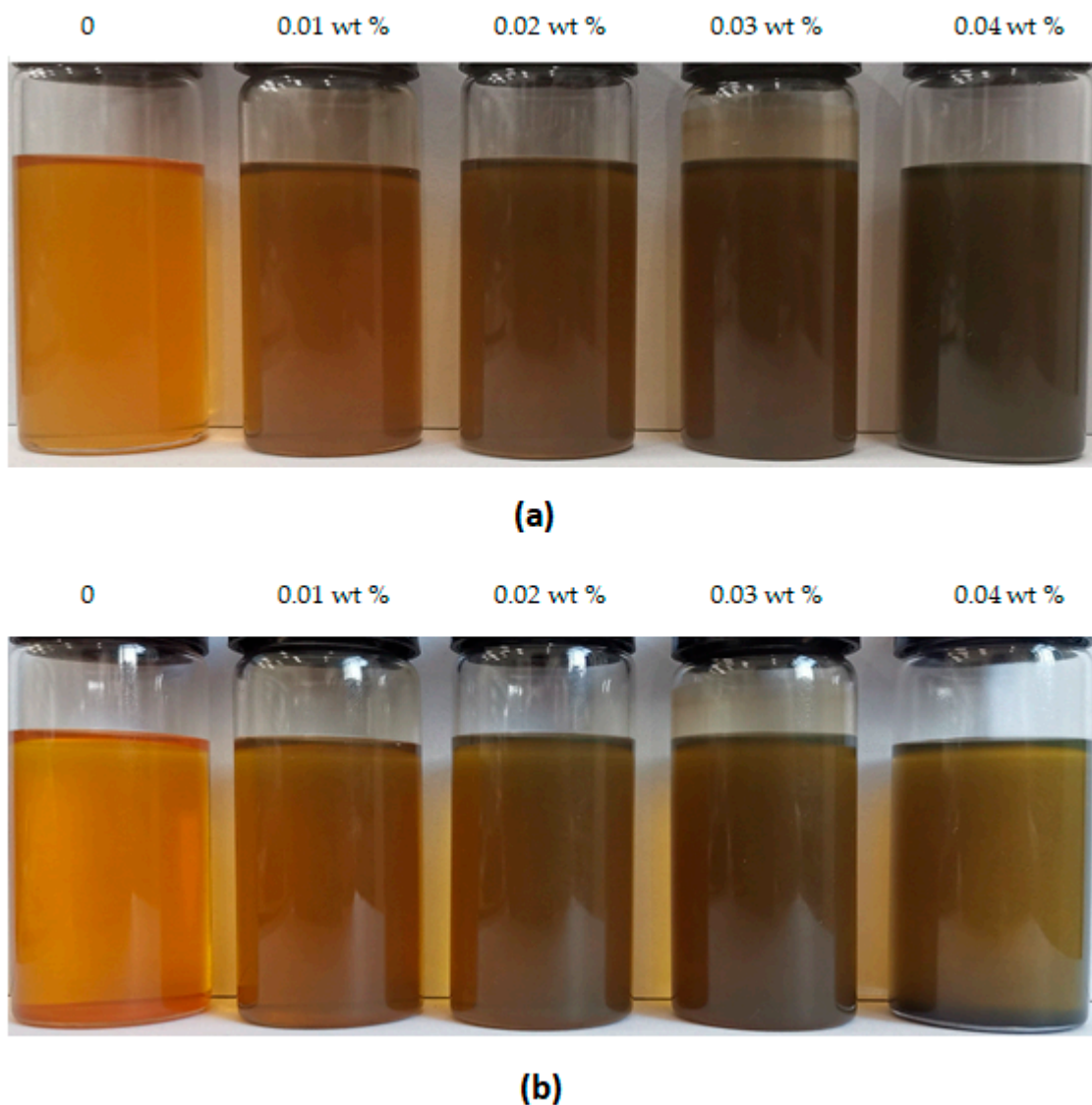


Figure 7. Digital images of 0# diesel oil (oil sample 1) with different concentrations of graphene additives settled for (a) 0 days and (b) 20 days.

3.4. Physical and Chemical Property Tests

The physical and chemical properties of fuel directly affect its storage, transportation, combustion, and emission. It was necessary to analyze whether the fuel characteristics met the standard GB252-2015. The physical and chemical properties of 0# diesel oil (oil

sample 1 and oil sample 2) with and without 0.03 wt % graphene lubrication additives were measured. The results are presented in Table 2.

Table 2. Physical and chemical properties of fuel oil samples (GB252-2015).

Fuel Oil Type	Sulfur Content (mg/kg)	Closed Flash Point (°C)	Kinematic Viscosity (20 °C) (mm ² /s)	Calorific Value (kJ/kg)
0# diesel oil (oil sample 1)	310	66	4.7998	45,693
0# diesel oil (oil sample 1) with 0.03 wt % graphene additive	310	68	4.8279	45,876
0# diesel oil (oil sample 2)	1.1	72	3.06	10,896
0# diesel oil (oil sample 2) with 0.03 wt % graphene additive	1.1	73	3.10	11,068
Standard (0# diesel oil) (GB252-2015)	<0.1% (IMO)	>55	3~8	>42,652

3.5. Atomization Performance Tests

The plunger-sleeve assembly, the delivery valve–valve seat assembly, and the injector needle valve–valve seat assembly of the fuel pump are all precision assemblies. As a solid lubricant additive in 0# diesel oil, graphene should not cause the jam between the plunger and the sleeve as well as the blocking in injection hole of the injector, which affects the atomization effect. The atomization performance tests of 0# diesel oil (oil sample 1 and oil sample 2) with and without 0.03 wt % graphene lubricant additives were carried out. The results are shown in Figure 8. The shape of the oil beams of the two oil samples were foggy, no obvious oil droplets or unevenness of the oil beam were observed, and the injection of fuel was crisp, which indicated that the atomization effect of 0# diesel oil (oil sample 1 and oil sample 2) with 0.03 wt % graphene lubricant additives was not reduced compared to pure 0# diesel oil (oil sample 1 and oil sample 2).

3.6. The Effect of Graphene Additive on the Lubricity of 0# Diesel Oil

The graphene additives were applied to 0# diesel oil (oil sample 1 and oil sample 2), and the lubricity of the graphene additives to 0# diesel oil (oil sample 1 and oil sample 2) were evaluated by WSD and COF.

3.6.1. Anti-friction Behavior

Figure 9 shows the average friction coefficient (COF) of 0# diesel oil (oil sample 1 and oil sample 2) with different concentrations of graphene additive (0, 0.01, 0.02, 0.03, 0.04, 0.05, and 0.06 wt %). The COF of pure oil sample 2 was higher than that of pure oil sample 1. This can be attributed to the removal of polar components such as organic nitrides and organic oxides that have lubrication properties while desulfurization, which reduces the lubricating properties of low-sulfur fuel [31]. Obviously, compared with pure 0# diesel oil (oil sample 1 and oil sample 2), the COF of 0# diesel oil (oil sample 1 and oil sample 2) containing different concentrations of graphene additives was reduced, however, 0# diesel oil (oil sample 1 and oil sample 2) containing 0.03 wt % graphene additive obtained the smallest friction coefficient (reduced by 20% and 24% compared with pure 0# diesel oil 1 and pure oil sample 2, respectively). This was because the contact area between the friction surfaces was related to the surface asperities. These phenomena benefit from the special structure of graphene. The smooth surface and the ultra-thin sheet structure of graphene make it easy to fill in the valleys between asperities. The contact area of the friction pair was decreased and the friction coefficient was reduced. However, when the graphene additives in 0# diesel oil (oil sample 1 and oil sample 2) reached a certain concentration, the graphene additives that entered the contact surface were saturated. As the concentration of graphene additives further increase, graphene may agglomerate, resulting in increased friction. When the graphene additives on the contact surface are saturated, the optimal

concentration is 0.03 wt %. Thence, graphene additives enhanced the antifriction property of 0# diesel oil (oil sample 1 and oil sample 2) owing to the formation of tribofilm on the contact surfaces. The small lamellar structure of graphene additives may more easily enter the contact surface of friction pairs to form a layer of anti-friction protective film. The protective film effectively prevents direct contact between metal asperities and significantly reduces friction.

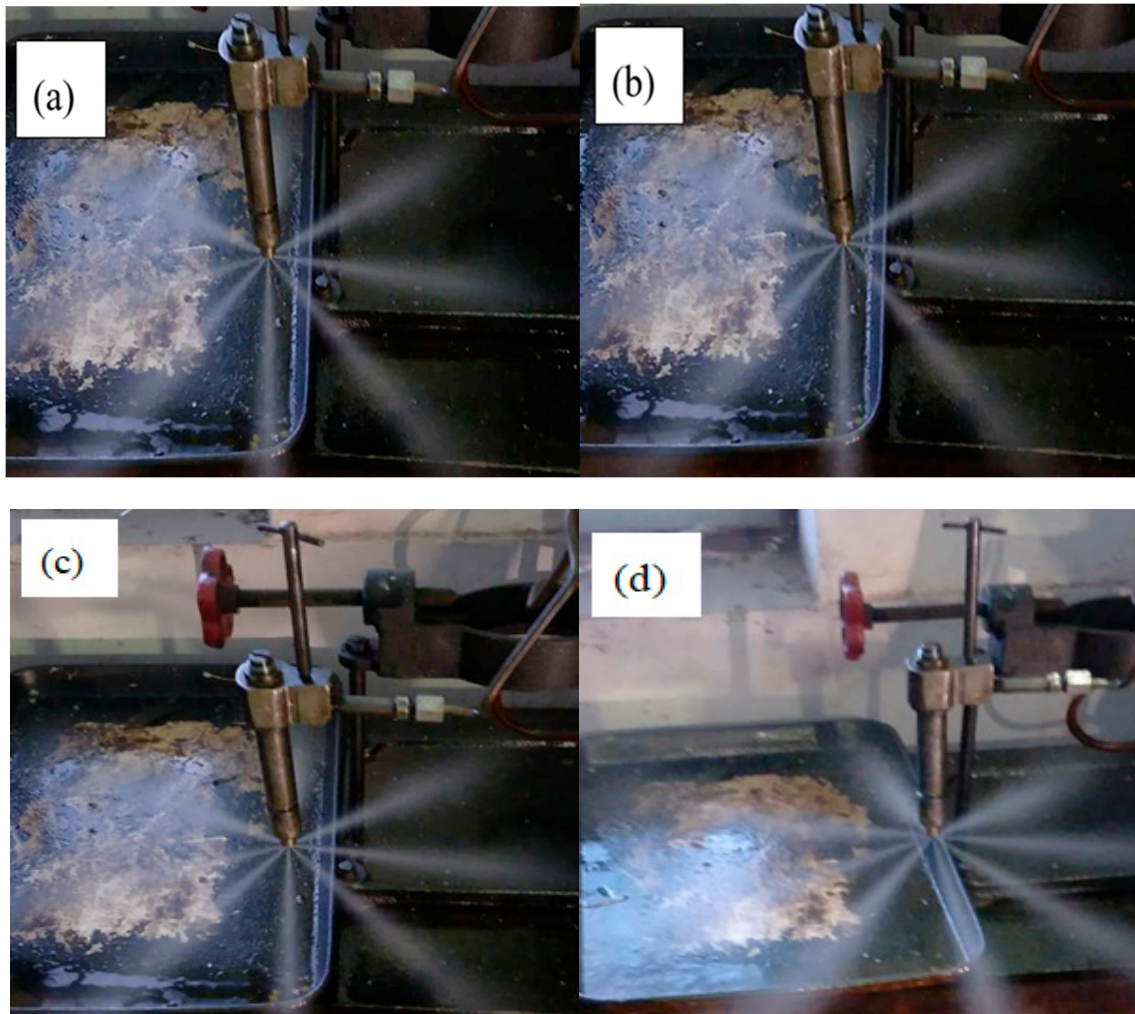


Figure 8. Atomization properties tests of (a) 0# diesel oil (oil sample 1); (b) 0# diesel oil (oil sample 1) with 0.03 wt % graphene additives; (c) 0# diesel oil (oil sample 2); (d) 0# diesel oil (oil sample 2) with 0.03 wt % graphene additives.

3.6.2. Anti-Wear Behavior

In order to assess anti-wear performances of graphene additives, we investigated the wear scar diameters (WSD) of the steel balls. Figure 10 shows the wear volume of 0# diesel oil (oil sample 1 and oil sample 2) with different concentrations of graphene additives (0, 0.01, 0.02, 0.03, 0.04, 0.05, and 0.06 wt %). As shown in Figure 10, the WSD decreased first and then increased with the increase of additive concentration. The 0# diesel oil (oil sample 1 and oil sample 2) with 0.03 wt % graphene additive obtained the minimum WSD, and the minimum WSD was reduced by 30% and 28% compared with pure 0# diesel oil 1 and pure oil sample 2, respectively). The optical micrograph (Figure 11) of the worn surface of the steel balls nicely confirmed the previous results. Obviously, the scratches of the steel ball lubricated with pure 0# diesel oil (oil sample 1 and oil sample 2) were wider and deeper than those of the steel ball lubricated with graphene additives. This shows that graphene

additives can greatly improve the anti-wear performance of 0# diesel oil (oil sample 1 and oil sample 2). The main reason for the decrease in the WSD was the formation of graphene friction film on the wear surface, which was an ultra-thin surface coating that can increase the load-carrying capacity, reduce the shear effect, and ultimately reduce the wear of the steel balls.

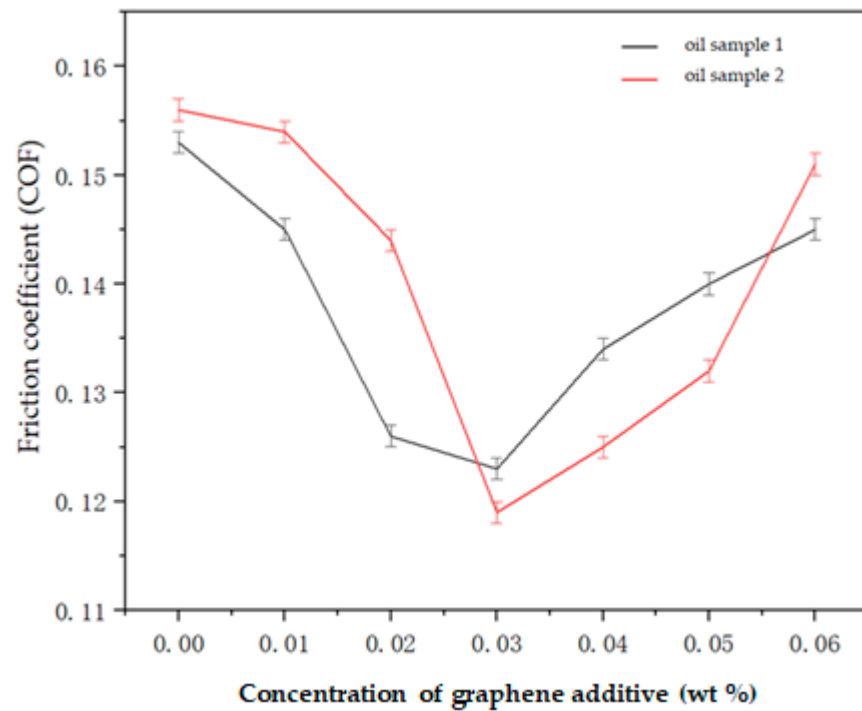


Figure 9. The friction coefficient curves of 0# diesel oil (oil sample 1 and oil sample 2) with different concentrations of graphene additive.

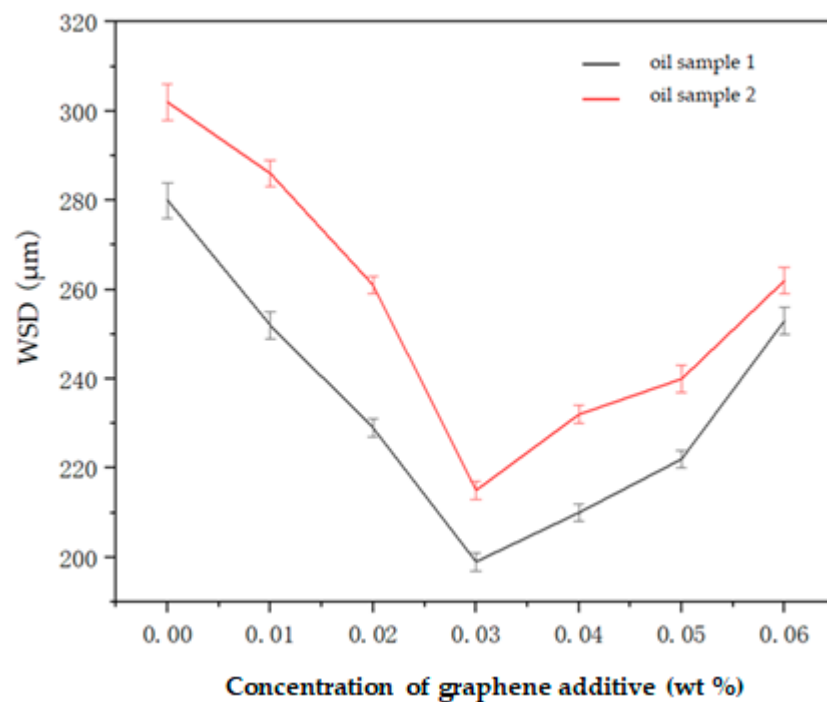


Figure 10. The wear scar diameter (WSD) of 0# diesel oil (oil sample 1 and oil sample 2) with different concentrations of graphene additive.

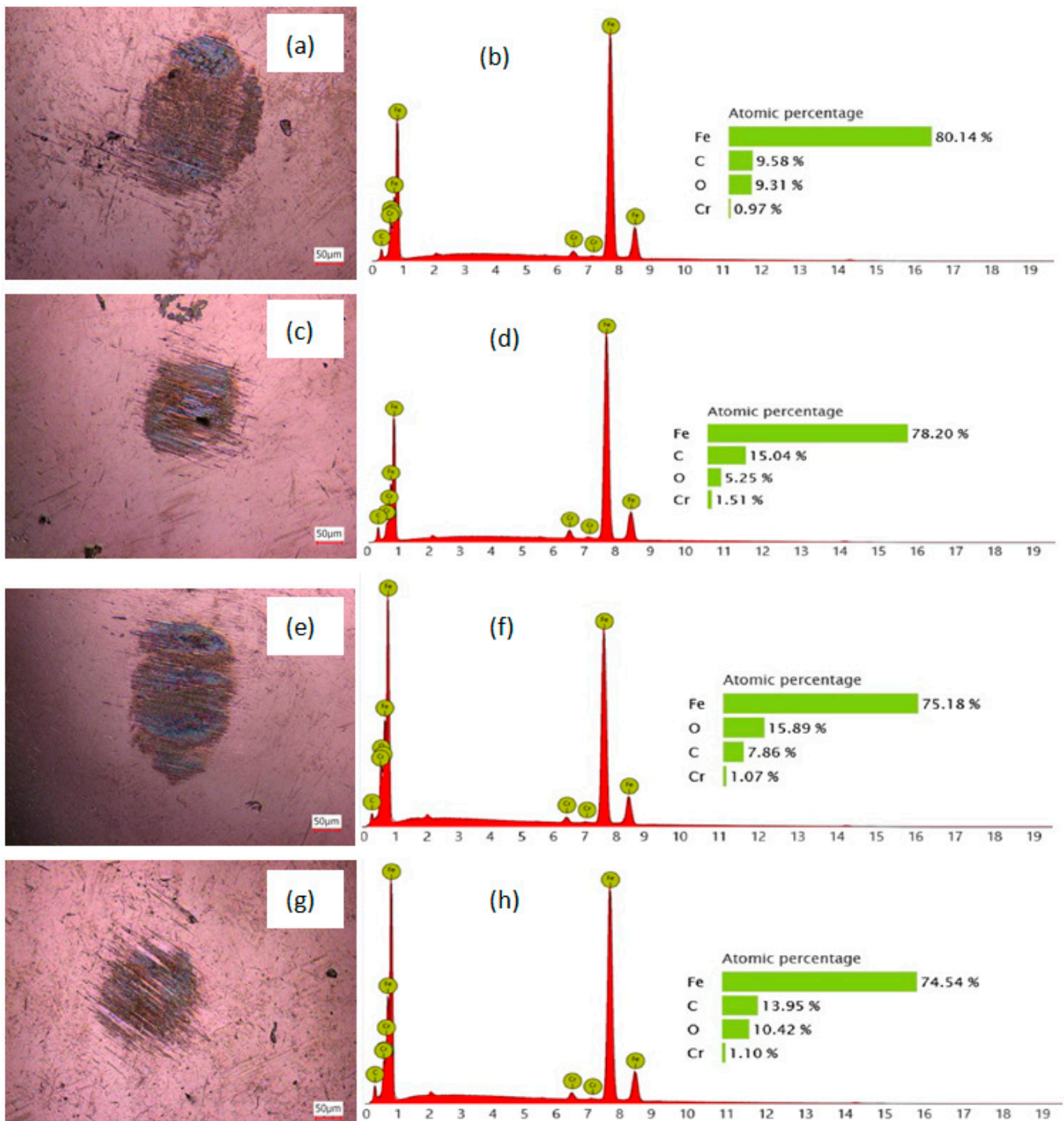


Figure 11. The optical micrograph of steel ball worn surfaces of friction pair and energy-dispersive spectroscopy (EDS) patterns of the steel disc worn surfaces of friction pair. (a,b) Lubricated by oil sample 1; (c,d) lubricated by oil sample 1 with 0.03 wt % graphene additives; (e,f) lubricated by oil sample 2; (g,h) lubricated by oil sample 2 with 0.03 wt % graphene additives.

3.6.3. Analysis of the Anti-Friction/Wear Mechanisms

Figure 11 shows the optical micrograph of the worn surfaces on steel balls lubricated with pure 0# diesel oil (oil sample 1 and oil sample 2) and compound oil containing 0.03 wt % graphene additives. As shown in Figure 11a,e, some severe adhesion phenomena occurred due to the loss of the tribofilm on the steel ball worn surfaces. The EDS patterns of

the steel disc worn surfaces are provided in Figure 11b,d,f,h. Obviously, the worn surface lubricated with compound oil containing 0.03 wt % graphene additive had a higher C than the worn surface lubricated with pure 0# diesel oil. This showed that self-lubricating film formed on the worn surface was thicker because of the addition of graphene additives into 0# diesel oil. This explains the increase in COF and WSD when using 0# diesel oil (oil sample 1 and oil sample 2) alone (Figures 9 and 10). When 0# diesel oil contains graphene additives, the adhesion phenomena of the steel ball surfaces were greatly reduced. This can be attributed to the formation of graphene friction film, which prevents the friction pair surface from contacting directly. Graphene possesses an extremely thin laminated structure, low shear stress, and high load-carrying capacity. These ensure that graphene can easily enter the rubbing surfaces and form a low-shear, high durability oil film to prevent direct metal to metal contacts, which results in the reduction of friction and wear. Therefore, graphene additives effectively improve the lubrication performance of 0# diesel oil (oil sample 1 and oil sample 2).

4. Conclusions

In this study, a simple, economical, and pollution-free method was introduced in order to prepare graphene lubricant additives for 0# diesel oil by dielectric barrier discharge plasma-assisted ball milling. The 0# diesel oil without any other chemical components was conducted as a modifier for the first time. A group of experimental studies were carried out on the high-frequency reciprocating rig (HFRR). The physical, chemical, and tribological properties of 0# diesel oil with graphene lubricant additives were investigated. The following conclusions can be drawn:

(1) The preparation and surface modification of graphene lubricant additives were completed in one step. Owing to the synergism of plasma thermal explosion effect, ball milling mechanical impact effect, and fuel oil cavitation effect, the expanded graphite was rapidly exfoliated and refined into graphene sheets with nine layers.

(2) Graphene lubricant additives had good compatibility with 0# diesel oil. During DBDP-assisted ball milling, reactions such as gasification, ionization, or cracking of molecular bonds occurred with low sulfur fuel, and many organic functional groups (-OH, C=C, -CH₂, -CH₃) were produced—these organic functional groups were adsorbed or polymerized on the surface of the graphene sheets, and the hydrocarbon long chain structure similar to that of 0# diesel oil was formed on the surface of graphene sheets.

(3) Graphene lubricant additives greatly improved the lubrication performance of 0# diesel oil. The addition of 0.03 wt % graphene resulted in 20% reduction in the COF and 28% reduction in WSD compared to pure 0# diesel oil with a sulfur content of 310 mg/kg. The addition of 0.03 wt % graphene resulted in 24% reduction in the COF and 30% reduction in WSD compared to pure 0# diesel oil with a sulfur content of 1.1 mg/kg. The principal reason was the formation of graphene tribofilm on the worn surfaces.

Author Contributions: Conceptualization, X.H. and L.D.; methodology, Y.M.; software, Y.W.; validation, X.H. and Y.M.; formal analysis, H.L.; investigation, X.H.; resources, Y.M.; data curation, Z.Y.; writing—original draft preparation, X.H.; writing—review and editing, G.B.; visualization, X.H.; supervision, L.D.; project administration, L.D.; funding acquisition, L.D. All authors have read and agreed to the published version of the manuscript.

Funding: This research was funded by National Natural Science Foundation of China [51779103], Science and Technology Key Project of Fujian Province [2018H0026], Natural Science Foundation of Fujian Province [2019J01708], Open Project Fund of Fujian Shipping Research Institute of Jimei University and Beibu Gulf University 2018 school-level research project [2018KYQD22].

Institutional Review Board Statement: Not applicable.

Informed Consent Statement: Informed consent was obtained from all subjects involved in the study.

Data Availability Statement: All data used to support the findings of this study are included within the article.

Acknowledgments: This work was financially supported by National Natural Science Foundation of China (51779103), Science and Technology Key Project of Fujian Province (2018H0026), Natural Science Foundation of Fujian Province (2019J01708), Open Project Fund of Fujian Shipping Research Institute of Jimei University and Beibu Gulf University 2018 school-level research project [2018KYQD22].

Conflicts of Interest: The authors declare that they have no conflict of interest regarding the publication of this paper.

References

1. Ye, L.; Wang, H.; Jiang, W. Analysis of the EAR conversion method for air pollutant emission concentration. *Energy Rep.* **2020**, *6*, 402–406. [\[CrossRef\]](#)
2. Zhang, Z.; Ye, J.; Tan, D.; Feng, Z.; Luo, J.; Tan, Y.; Huang, Y. The effects of Fe₂O₃ based DOC and SCR catalyst on the combustion and emission characteristics of a diesel engine fueled with biodiesel. *Fuel* **2021**, *290*, 120039. [\[CrossRef\]](#)
3. Wang, Z.; Zhang, H.; Gan, X. Research on Solution of Ship Low Sulphur Fuel based on IMO Sulphur Limitation Regulation. In Proceedings of the 2019 3rd International Conference on Environmental, Industrial and Energy Engineering (EI2E 2019), Yinchuan, China, 19–21 September 2019.
4. Nicolau, A.; Lutckmeier, C.V.; Samios, D.; Gutierrez, M.; Piatnick, C.M. The relation between lubricity and electrical properties of low sulfur diesel and diesel/biodiesel blends. *Fuel* **2018**, *117*, 26–32. [\[CrossRef\]](#)
5. Hong, F.T.; Alghamdi, N.M.; Bailey, A.S.; Khawajah, A.; ManiSarathy, S. Chemical and kinetic insights into fuel lubricity loss of low-sulfur diesel upon the addition of multiple oxygenated compounds. *Tribol. Int.* **2020**, *152*, 106559. [\[CrossRef\]](#)
6. Hu, Z.; Zhang, L.; Li, Y. Investigation of tall oil fatty acid as antiwear agent to improve the lubricity of ultra-low sulfur diesels. *Tribol. Int.* **2017**, *114*, 57–64. [\[CrossRef\]](#)
7. Alves, S.M.; de Farias, A.C.M.; Mello, V.S.; Oliveira Junior, J.J. Effect of soybean biodiesel addition on tribological performance of ultra-low sulfur diesel. *J. Tribol. Trans. ASME* **2019**, *141*, 2–5. [\[CrossRef\]](#)
8. Tomic, M.; Savin, L.; Micic, R. The Possibility of using biodiesel oil from sunflower oil as an additive for the improvement of lubrication properties of low sulfur diesel fuel. *Energy* **2014**, *65*, 101108. [\[CrossRef\]](#)
9. Sun, L.; Li, M.; Ma, C.; Li, P. Preparation and evaluation of Jatroph acurc as based catalyst and functionalized blend components for low sulfur diesel fuel. *Fuel* **2017**, *206*, 27–33. [\[CrossRef\]](#)
10. Liu, Z.; Li, J.; Knothe, G.; Sharma, B.K.; Jiang, J. Improvement of diesel lubricity by chemically modified tung-oil based fatty acid esters as additives. *Energy Fuels* **2019**, *33*, 5110–5115. [\[CrossRef\]](#)
11. Chouhan, A.; Mungse, H.P.; Khatri, O.P. Surface chemistry of graphene and graphene oxide: A versatile route for their dispersion and tribological applications. *Adv. Colloid Interface Sci.* **2020**, *283*, 102215. [\[CrossRef\]](#)
12. Jason, Y.J.J.; How, H.G.; Teoh, Y.H.; Chuah, H.G. A Study on the Tribological Performance of Nanolubricants. *Processes* **2020**, *8*, 1372. [\[CrossRef\]](#)
13. Demirtas, S.; Kaleli, H.; Khadem, M.; Kim, D. Tribotest of engine piston ring/cylinder liner pairs with different nanoparticles added into engine oil. *Ind. Lubr. Tribol.* **2020**, *72*, 217–231. [\[CrossRef\]](#)
14. Wang, X.; Zhang, Y.; Yina, Z.; Su, Y.; Zhang, Y.; Cao, J. Experimental research on tribological properties of liquid phase exfoliated graphene as an additive in SAE 10W-30 lubricating oil. *Tribol. Int.* **2019**, *135*, 29–37. [\[CrossRef\]](#)
15. Gayatri, P.; Subhasis, S.; Harish, H.; Tapas, K.; Murmu, N.C. Tribological behavior of dodecylamine functionalized graphene nanosheets dispersed engine oil nanolubricants. *Tribol. Int.* **2019**, *131*, 605–619.
16. Dai, L.Y.; Meng, R.G.; Chen, J.F. Preparation and Application of Surface Modified Nano Materials as Lubricating Oil Additives. Patent CN103804960A, 21 May 2014.
17. Yan, J.; Dai, L.Y.; Meng, R.G. Tribological properties of surface modified nano-TiO₂ prepared by plasma assisted ball milling. *Tribology* **2016**, *36*, 20–26.
18. Wei, W.; Yang, S.; Zhou, H.X.; Lieber Wirth, I.; Feng, X.L.; Mullen, K. 3D graphene foams cross-linked with pre-encapsulated Fe₃O₄ nanospheres for enhanced lithium storage. *Adv. Mater.* **2013**, *25*, 2909–2914. [\[CrossRef\]](#)
19. Jaleh, B.; Khalilipour, A.; Habibi, S.; Niyafar, M.; Nasrollahzadeh, M. Synthesis, characterization, magnetic and catalytic properties of graphene oxide/Fe₃O₄. *J. Mater. Sci. Mater. Electron.* **2016**, *28*, 4974–4983. [\[CrossRef\]](#)
20. Lin, C.; Yang, L.; Ouyang, L.; Liu, J.; Wang, H.; Zhu, M. A new method for few-layer graphene preparation via plasma-assisted ball milling. *J. Alloy. Compd.* **2017**, *728*, 578–584. [\[CrossRef\]](#)
21. Pol, V.G.; Shrestha, L.; Kumar, A.K. Tunable, functional carbon spheres derived from rapid synthesis of resorcinol-formaldehyde resins. *ACS Appl. Mater. Interfaces* **2014**, *6*, 10649–10655. [\[CrossRef\]](#)
22. Sun, J.; Liu, H.M.; Chen, X.; Evans, D.G.; Yang, W.S.; Duan, X. Synthesis of Graphene Nanosheets with Good Control over the Number of Layers Within the Two-Dimensional Galleries of Layered Double Hydroxides. *Chem. Commun.* **2012**, *48*, 8126–8128. [\[CrossRef\]](#)
23. Ren, B.J.; Gao, L.; Li, M.J.; Zhang, S.D.; Zu, G.Q.; Ran, X. Tribological properties and anti-wear mechanism of ZnO @ graphene core-shell nanoparticles as lubricant additives. *Tribol. Int.* **2020**, *144*, 106114. [\[CrossRef\]](#)
24. Liu, H.; Li, Y.Q.; Wang, T.M.; Wang, Q.H. In situ synthesis and thermal, tribological properties of thermosetting polyimide/graphene oxide nanocomposites. *J. Mater. Sci.* **2012**, *47*, 1867–1874. [\[CrossRef\]](#)

25. Li, Y.Q.; Wang, Q.H.; Wang, T.M.; Pan, G.Q. Preparation and tribological properties of graphene oxide/nitrile rubber nanocomposites. *J. Mater. Sci.* **2012**, *47*, 730–738. [[CrossRef](#)]
26. Zhang, L.; He, Y.; Zhu, L. Alkyl phosphate modified graphene oxide as friction and wear reduction additives in oil. *J. Mater. Sci.* **2019**, *54*, 4626–4636. [[CrossRef](#)]
27. Askariana, M.; Vatani, A.; Edalata, M. Heavy oil upgrading via hydrodynamic cavitation in the presence of an appropriate hydrogen donor. *J. Pet. Sci. Eng.* **2017**, *151*, 55–61. [[CrossRef](#)]
28. Gevari, M.T.; Abbasiasl, T.; Niazi, S.; Ghorbani, M.; Kosar, A. Direct and indirect thermal applications of hydrodynamic and acoustic cavitation: A review. *Appl. Therm. Eng.* **2020**, *171*, 115065. [[CrossRef](#)]
29. Li, L.; Chen, Y.; Behan, G.; Zhang, H.; Petravic, M.; Glushenkov, A.M. Large-scale mechanical peeling of boron nitride nanosheets by low-energy ball milling. *J. Mater. Chem.* **2011**, *21*, 11862–11866. [[CrossRef](#)]
30. Leroux, F.; Campagne, C.; Perwuelz, A. Polypropylene film chemical and physical modifications by dielectric barrier discharge plasma treatment at atmospheric pressure. *J. Colloid Interface Sci.* **2008**, *328*, 412–420. [[CrossRef](#)]
31. Hsieh, P.Y.; Bruno, T.J. A perspective on the origin of lubricity in petroleum distillate motor fuels. *Fuel Process Technol.* **2015**, *129*, 52–60. [[CrossRef](#)]